Welding of 42SiCr High-Strength Steel

Michal Peković, Štěpán Jeníček, Kateřina Rubešová, Ivan Vorel, Hana Jirková
Faculty of Mechanical Engineering – Regional Technological Institute, University of West Bohemia,
Univerzitní 8, 306 14 Pilsen, Czech Republic
E-mail: pekovicm@rti.zcu.cz, jeniceks@rti.zcu.cz, krubesov@rti.zcu.cz, frost@rti.zcu.cz, hstankov@rti.zcu.cz

Various industry sectors are using advanced high-strength steels nowadays. Application of these steels are often constrained by the capabilities of their manufacturing and processing technologies. To deliver the required properties, advanced high-strength steels must possess the prescribed microstructures which can be achieved by specific heat treatment routes, such as intercritical annealing or the Q&P process. Difficulties, however, arise in these materials' joining, and welding in particular. Welding profoundly affects the microstructure and mechanical properties of the product due to the amount of heat input and subsequent rapid cooling. For these reasons, laser welding and electron beam welding tests were carried out on experimental 42SiCr steel. Prior to welding, the material was treated using two different Q&P process sequences and one conventional quenching sequence. The weld metal, the heat affected zone and the base material were examined by metallographic methods and the impact of the introduced heat on the microstructure was studied.

Keywords: welding, laser, electron beam, AHSS steel, mechanical tests

1 Introduction

The demand for new materials, including advanced high-strength steels (AHSS), has been growing recently. A majority of these steels are of the multiphase type, delivering much better combinations of mechanical properties and weight savings than conventional materials [1]. Typical representatives of these advanced high-strength steels are Q&P-processed martensitic steels. Q&P process is a heat treatment method which comprises two steps. During these steps, the steel is quenched from the austenitizing temperature to a temperature between the martensite start and martensite finish temperatures. Afterwards, it is reheated to a partitioning temperature, which is equal to or higher than the martensite start temperature, and held at this temperature. During holding, carbon migrates from super-saturated martensitic laths into austenite. As austenite becomes enriched with carbon, it becomes more stable. The stabilised austenite improves the ductility of Q&P steels. Q&P-processed steels can show final tensile strengths of up to 2000 MPa, along with high elongation of up to 20%. Although these values are very favourable, no technologies for producing safe and reliable joints are known today which do not degrade the properties of the parts joined [2, 3].

An example of these methods is fusion welding [4]. Promising methods also include welding by a beam of particles. The first one is laser beam welding. It effectively produces welds of good quality. Using this method, relatively wide gaps can be filled. The post-welding cooling is slower than in conventional welding methods, due to lower welding speeds and a larger amount of heat introduced. [5] Electron beam welding has been known for more than 60 years but only recent years have seen a rising interest from industry and science. The method is characterized by an extremely high energy density of the beam. High welding speed results in a very narrow heat-affected zone. Electron beam welding can create joints in materials which would be unweldable by conventional methods. As electron beam welding is performed in vacuum, the size of the vacuum chamber limits the parts' size. [6]

2 Experimental methods

The purpose of this experiment was to create weld joints by laser and electron beams. The parts were prepared by Q&P processing and conventional quenching. Low-alloy 42SiCr steel was selected as the experimental material (Tab. 1). The main alloying elements of the material were manganese, silicon and chromium, beside carbon. Owing to this chemistry, the Q&P process produces martensitic microstructures with retained austenite and the carbide precipitation is strongly suppressed. [7]

Tab. 1 *Chemical composition of experimental steel [wt%]*

	C	Si	Mn	Cr	Mo	Nb	S	P
42SiCr	0.42	2.03	0.56	1.33	0.16	0.03	0.003	0.005

Heat treatment was carried out in a furnace with no protective atmosphere (Fig. 1). First, the material was quenched (the KAL sequence): heating to 950°C and quenching in water. Then the experimental steel was Q-P processed. Sequence 2 (QP1) comprised austenitizing at 950°C for 100 s, water quenching to 230°C and partitioning at 380°C for 600 s. The third heat treatment sequence (QP2) involved a lower quenching temperature, 200°C, and partitioning at 250°C for 600 s (Fig. 1).

After heat treatment, the specimens were cut at mid-length, assembled and lap welds were made on them. The length of the overlap was 16 mm (Fig. 2, Fig. 3). The weld was C-shaped, as shown in the drawing of its geometry and dimensions in the right part of Fig. 2. The beams had a diameter of 0.4 mm.

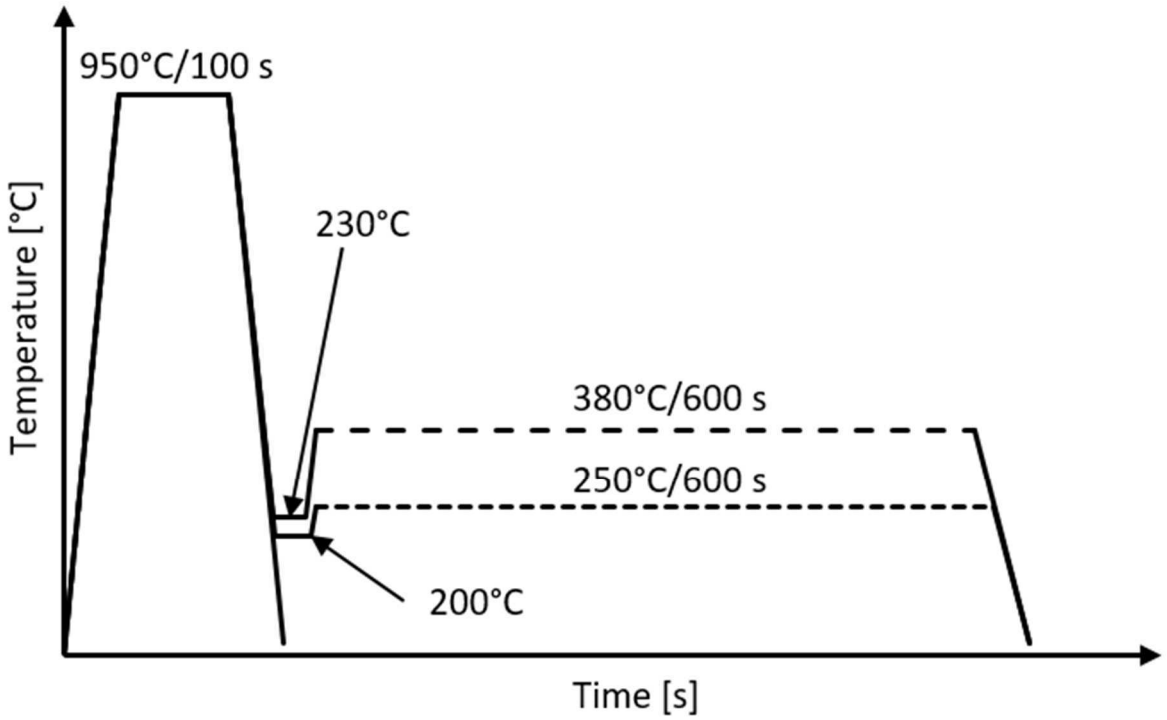

Fig. 1 *Diagram of heat treatment routes*

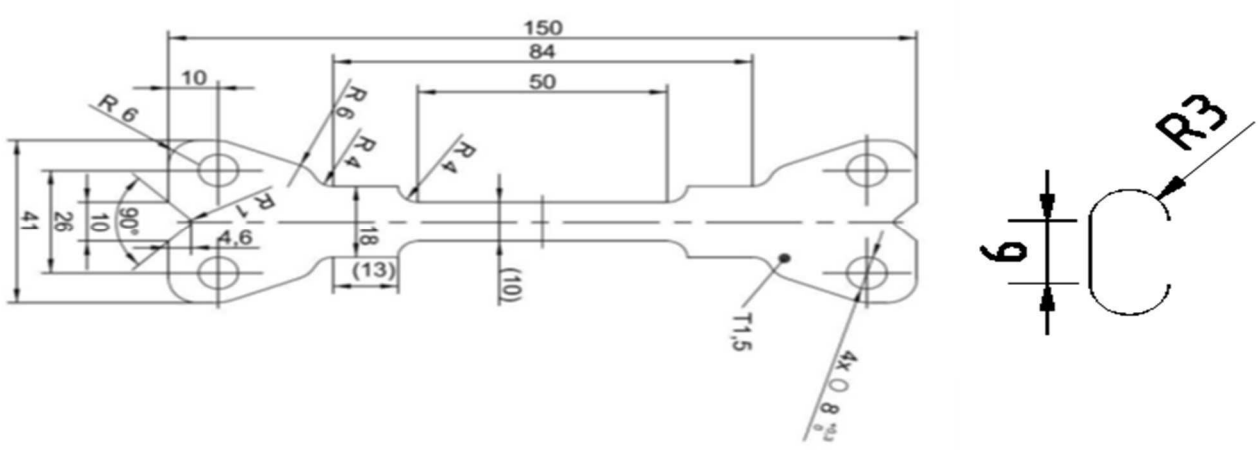

Fig. 2 *Drawing of the test specimen (left) and dimensions of the C-shaped weld (right)*

2.1 Laser beam welding

The Laserline LDF 5.000-40 fibre diode laser of up to 5 kW power was employed. After the process parameters were fine-tuned, the specimens were welded using the power of 1800 W. The speed was 25 mm/s. In all cases, the shielding gas was argon.

2.2 Electron beam welding

Fig. 3 *Specimens welded by laser beam (left) and electron beam (right)*

The MEBW-60 electron beam welding machine with the acceleration voltage interval of 5–60 kV and a maximum power of 2 kW was used. Fine-tuning of the parameters was the first step in the process. The welding power and speed were 630 W and 13 mm/s, respectively.

The amount of heat input governs the size of the heat-affected zone and its microstructure (Tab. 2). The values in the table were calculated from the following formulae:

$$Q_s = \frac{P}{1000 \cdot v_s}\left[kJ \cdot mm^{-1}\right] \quad (1)$$

$$Q_c = Q_s \cdot l\left[kJ\right] \quad (2)$$

Where:
Q_s ……specific heat input [kJ.mm^{-1}]
Q_c ……total heat input [kJ]
P ……welding power [W]
V_s ……welding speed [mm.s^{-1}]
l ……weld length [mm]

Tab. 2 Heat input in welding of experimental specimens

	Laser 1800	Electron beam
Specific heat input [kJ/mm]	0.072	0.048
Total heat input [kJ]	1.79	1.19

3 Results and discussion

Microstructures of the welded specimens were examined using optical and scanning electron microscopy. The sizes of heat-affected zones were measured. Mechanical properties were determined by HV0.1 hardness testing.

3.1 Evaluation of weld metal and heat-affected zone

The penetration varied with the welding method in this experiment. In the laser-welded specimens it was smaller than in the electron beam-welded ones. As for the weld shape, electron beam welding produced a wedge shape which was broader near the surface (Fig. 4, left). In laser welds, the portion near the surface was up to three times wider than the root (Fig. 4, right). In addition, shrinkage cavities and cracks were found in the laser welds. [8]

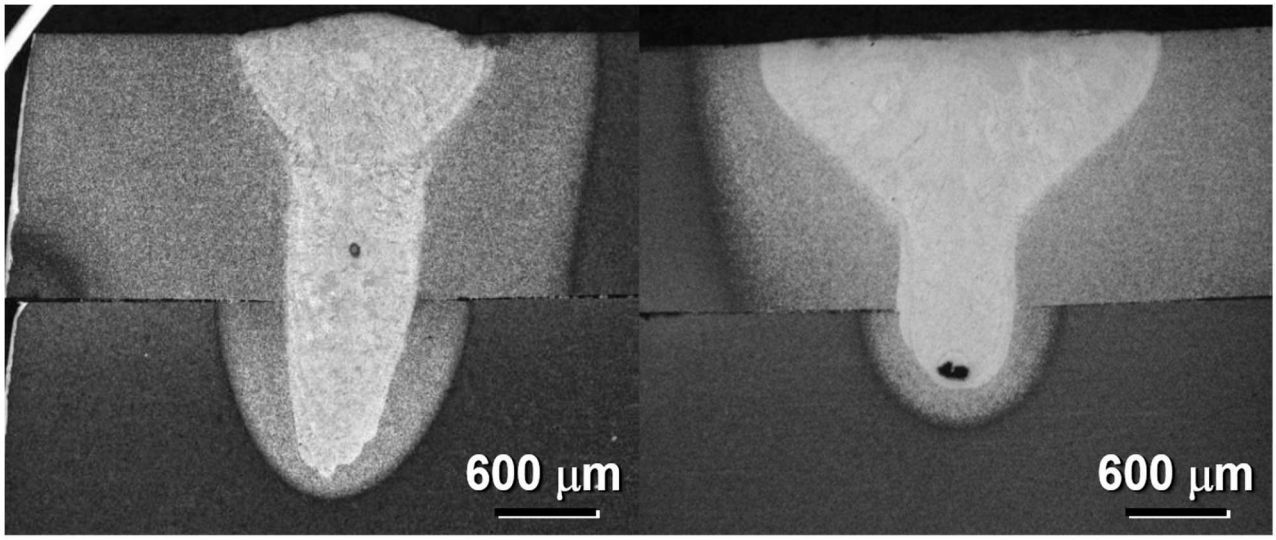

Fig. 4 *Cross sections through an electron beam weld (left) and a laser beam weld (right)*

There were differences in the surface condition of the welds as well. Laser welding with shielding gas produced an oxide layer. Electron beam welds made in vacuum showed no surface decarburization.

Tab. 3 Heat-affected zone widths

Heat-affected zone widths [mm]	Laser beam	Electron beam
KAL, longitudinal section	1.41	1.43
KAL, transverse section	1.03	0.93
QP1, longitudinal section	1.34	1.38
QP1, transverse section	1.03	0.97
QP2, longitudinal section	1.15	1.41
QP2, transverse section	0.89	0.97

Welding creates a heat affected zone adjacent to the weld. If the weld is sound (free from cracks and other defects), this zone is typically the weak spot of the entire welded joint. The size of this zone is governed mainly by the amount of the heat input and by the metal's heat dissipation capacity. Tab. 3 lists the heat-affected zone sizes measured on optical micrographs of longitudinal and transverse sections. [9] The width of the heat-affected zone was larger on longitudinal sections than on the transverse ones. The reason is the chosen weld shape.

3.2 Microhardness testing

The effect of heat dissipation from the heat-affected zone on microstructural evolution was evaluated by measuring microhardness profiles (Fig. 5). Vickers HV 0.1 values were acquired using the UHL VMHT microhardness tester. This measurement was only carried out on longitudinal cross sections. Indentations were spaced at 0.1 mm, forming a line from the weld centre to the base material.

Microhardness values showed no dependence on the welding method. Irrespective of the welding method and prior heat treatment, the hardness of the weld was approx. 700 HV0.1. Hardness values decreased with increasing distance from the weld. In the base material, they were 400–425 HV0.1, regardless of the prior heat treatment. This suggests that differences in heat treatment have no major effect on hardness.

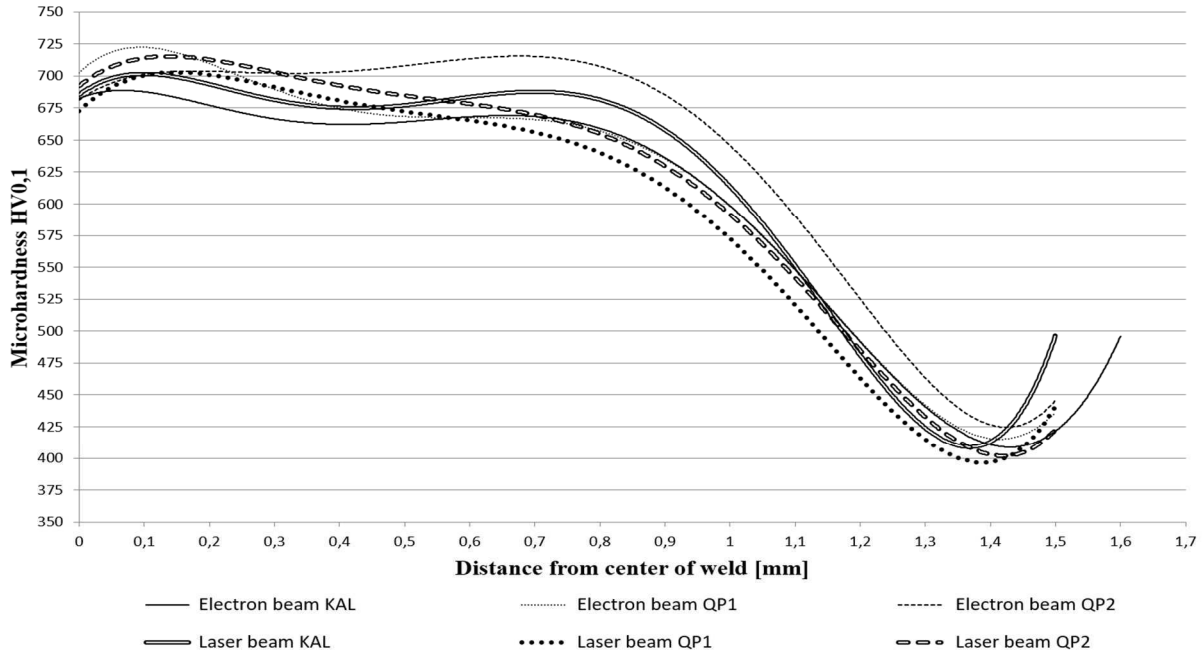

Fig. 5 *Microhardness profile plots vs. distance from the center of the weld*

The steepest decrease in hardness was found at the distance of 1–1.3 mm. This is the heat-affected zone, the transition between the weld metal and base material.

3.3 Microstructure analysis

Detailed examination of the welded specimens' microstructures was conducted with the aid of scanning electron microscopy. The specimens were ground, polished and etched with 3% nital solution. For greater accuracy, the microstructures were compared with micrograph in literature. [10, 11]

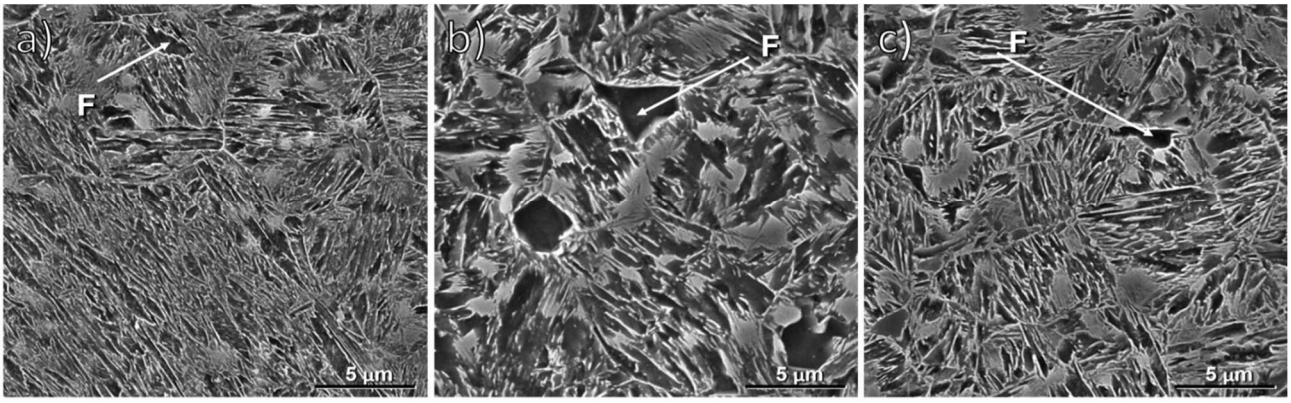

Fig. 6 *Microstructures after heat treatment a) KAL, b) QP1, c) QP2*

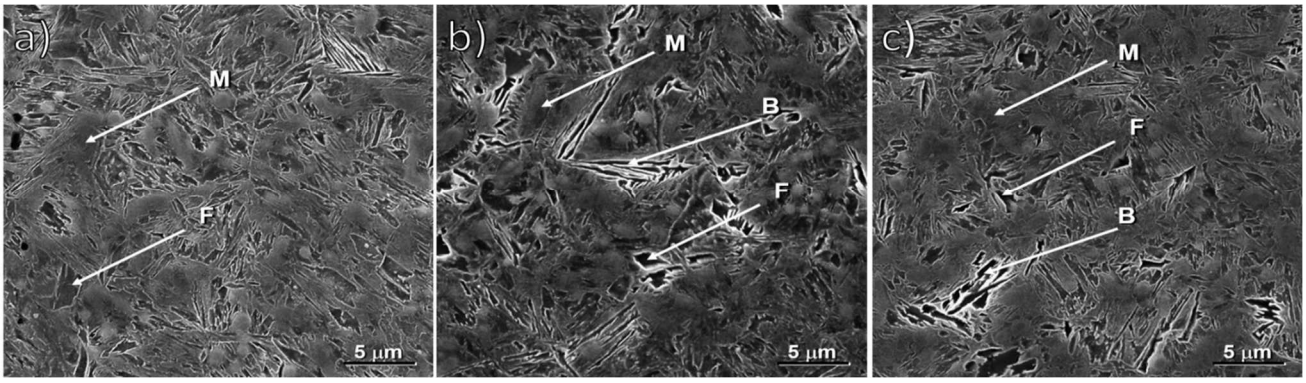

Fig. 7 *Heat affected zone upon electron beam welding. a) KAL, b) QP1, c) QP2*

Upon heat treatment, the microstructures consisted of martensite, bainite and retained austenite. Small amounts of free ferrite (F) were found as well. The finest microstructure was obtained by conventional quenching

(Fig. 6a). The QP1 sequence with the high partitioning temperature of 380°C produced a highly-tempered and coarsened microstructure (Fig. 6b). If the partitioning temperature had been lower, i.e. 250°C as in the QP2 sequence, the microstructure would have been more similar to the quenched microstructure (Fig. 6c). Nevertheless, a certain level of tempering can be found as well. No appreciable carbide precipitates were found in any case, which can be attributed to manganese and silicon alloying.

Heat-affected zones of electron beam-welded specimens contained very similar microstructures, regardless of the prior heat treatment (Fig. 7). They consisted of bainite (B), martensite (M) and a small fraction of ferrite. The same character of microstructure was preserved in the specimens. The specimen upon QP1 exhibited the coarsest structure.

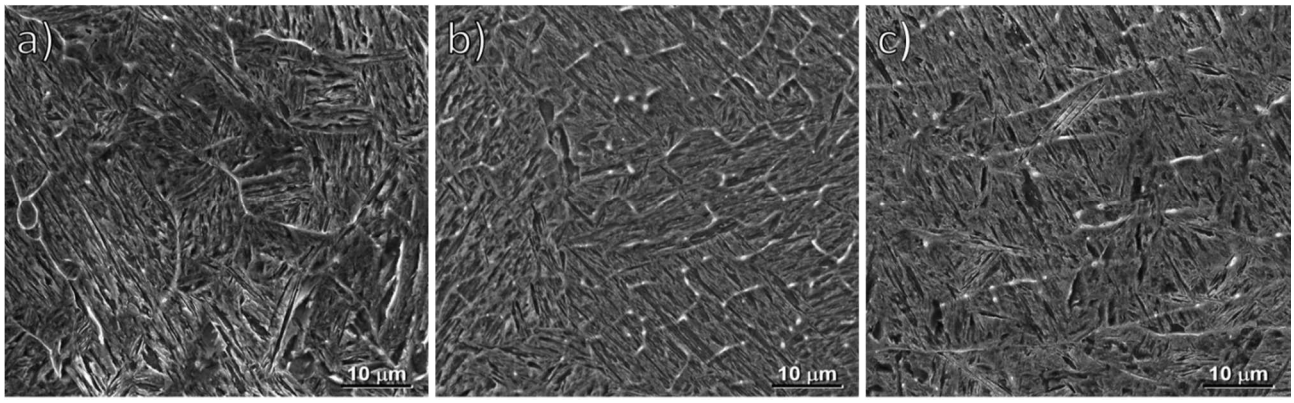

Fig. 8 *Weld area upon electron beam welding a) KAL, b) QP1, c) QP2*

The regions of weld joints produced by electron beam welding contained microstructures which were very different from the previous ones. They consisted predominantly of needle-like martensite (Fig. 8). The bainite fraction was very low. There were clear signs of dendritic segregation caused by melting. Differences in the microstructures of specimens with different heat treatment histories are probably down to the fact the micrographs were taken in other locations of the weld where cooling took place at different rates.

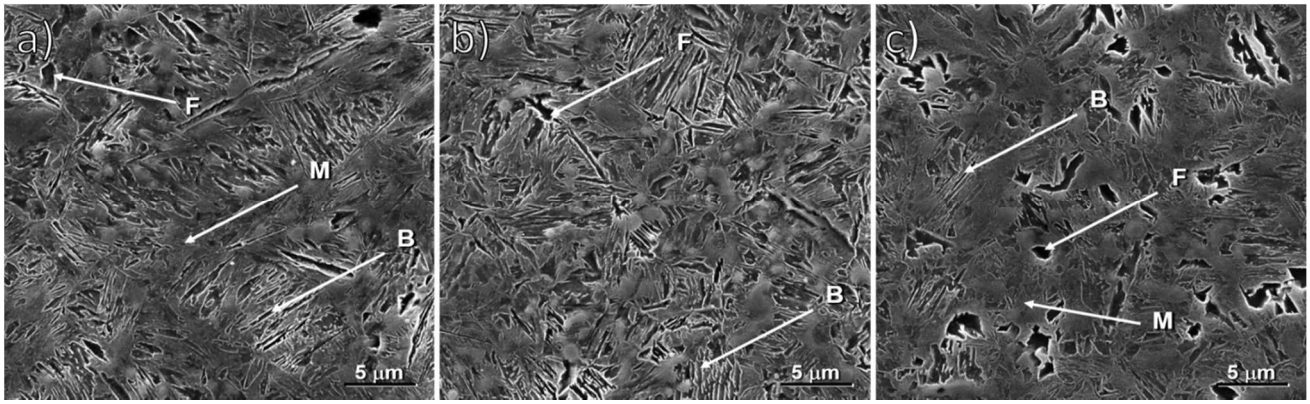

Fig. 9 *Heat affected zone upon laser beam welding a) KAL, b) QP1, c)QP2*

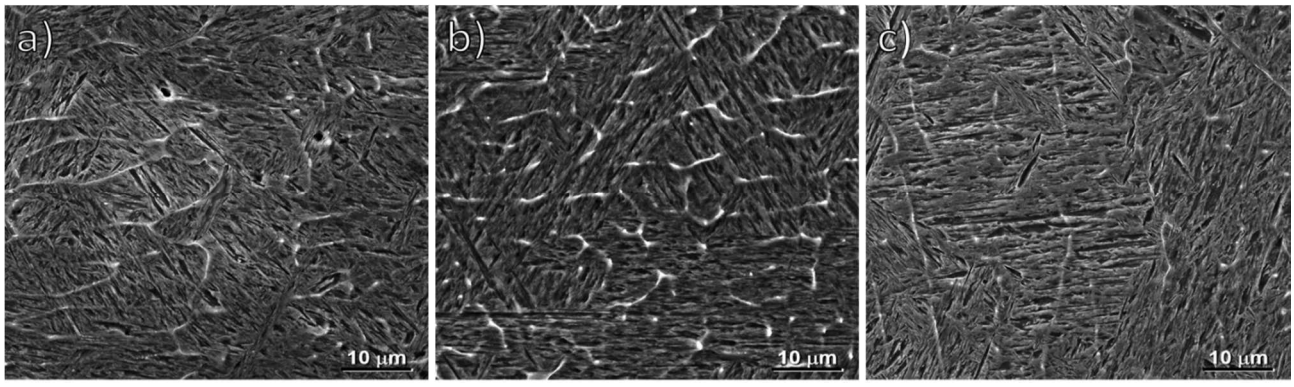

Fig. 10 *Weld area after laser beam welding a) KAL, b) QP1, c) QP2*

Heat-affected zones of laser welded joints were very similar in all cases (Fig. 9). The consisted of bainite sheaves, martensite needles and a small amount of ferrite. No carbide precipitates were found even in the bainite areas.

Laser welds contained needle-like martensite (Fig. 10). Again, there were clear signs of dendritic segregation

caused by melting.

Welding changed the character of the microstructure imparted by prior heat treatment in all cases. The welds typically contained martensite with no signs of high tempering. In the heat-affected zone, the bainite fraction increased above that existing upon heat treatment. All these changes were reflected in the changes in hardness. In the weld, hardness levels were higher than upon heat treatment: approx. 700 HV0.1. In the heat-affected zone, hardness gradually decreased to 400–425 HV0.1.

4 Conclusion

Specimens of 42SiCr steel with a martensitic-bainitic microstructure were welded by electron beam and laser. Prior to welding, the specimens were prepared by quenching and by a modern heat treatment route, Q&P processing. The purpose was to explore degradation and microstructural changes in the weld and the heat-affected zone.

After welding, metallographic examination and Vickers HV 0.1 microhardness testing were carried out. Indentations were spaced at 0.1mm, forming a profile from the weld centre to the base material. The values were very similar in all cases. In the center of the weld, they were approx. 700 HV 0.1, decreasing with increasing distance from the center to the level of 400–425 HV 0.1. This suggests that neither heat treatment nor the method of subsequent welding have any appreciable effect on microhardness.

Microstructure examination revealed no significant microstructural differences depending on heat treatment or welding method either. Prior to welding, the material consisted of highly-tempered martensite with a small amount of ferrite. The main difference was in their fineness, due to the partitioning temperature in the case of the Q&P-processed specimens. Heat-affected zones consisted of bainite and martensite and a small amount of ferrite. The only difference between them was in the fineness again, depending on the location of observation. The weld joint contained predominantly martensite. Furthermore, the microstructure showed notable signs of dendritic segregation due to melting.

Results of this experiment suggest that the method of welding used has no effect on differences in microstructural evolution or mechanical properties of 42SiCr steel. Furthermore, it can be stated that the only effect of heat treatment prior to welding is manifested in the fineness of the resulting microstructure, in both heat-affected zone and the weld joint.

Acknowledgement

The present contribution has been prepared under project LO1502 'Development of the Regional Technological Institute' under the auspices of the National Sustainability Programme I of the Ministry of Education of the Czech Republic aimed to support research, experimental development and innovation.

References

[1] KELLER, S. et al. (2014) WorldAutoSteel - Strong. Safe. Sustainable. In: *WorldAutoSteel.* Vol. 5

[2] EDMONDS, D. et al. (2006). Quenching and partitioning martensite-A novel steel heat treatment. In *Materials Science and Engineering A.* Vol. 438-440, No. 25, pp. 25-34

[3] WANG, C., SHI, J., CAO, W. DONG, H. (2010) Characterization of microstructure obtained by quenching and partitioning process in low alloy martensitic steel. In: *Materials Science and Engineering A.* Vol. 527, No. 15, pp. 3442-3449

[4] REISGEN, U. SCHLESER, M. MOKROV, O. AHMED, E. (2012) Statistical modeling of laser welding of DP/TRIP steel sheets. In: *Optics & Laser Technology.* Vol. 44, No. 1, pp. 92-101

[5] BAGGER, C. (2005) Review of laser hybrid welding. In: *Journal of laser applications*. Vol. 17, No. 1

[6] WĘGLOWSKI, M, St. BŁACHA. S. PHILLIPS, A. (2016) Electron beam welding – Techniques and trends – Review. In: *Vacuum*. Vol. 130, pp. 72-92

[7] KUČEROVÁ, L., JIRKOVÁ. H., KÁŇA, J., (2016) The Suitability of 42SiCr Steel for Quenching and Parti-tioning Process. In: *Manufacturing Technology*, Vol. 16, No. 5, pp. 984-989. ISSN 1213-2489

[8] VOREL, I., RUBESOVA, K., KHALAJ, O., OPATOVA, K., WAGNER, M. F. X., (2015) Analysis of Laser Welds on Steel Processed by Q-P Process. In: In: *4th International Conference on Advances in Mechanical, Aeronautical and Production Techniques.* pp. 29-32.

[9] VOREL, I., JENÍČEK, Š., KÁŇA, J., IBRAHIM, K, KOTĚŠOVEC, V., (2016) Use of Optical and Electron Mi-croscopy in Evaluating Optimization by Material-Technological Modelling of Manufacturing Processes In-volving Cooling of Forgings. In: *Manufacturing Technology*, Vol. 16, No. 6, pp. 1383-1387. ISSN 1213-2489

[10] VANDER VOORT, G. (2004) Metallography and microstructures. *ASM Handbook.* ASM International, Vol. 9

[11] SANTOFIMIA, M. J., ZHAO, L., SIETSMA, J., (2011) Overview of Mechanisms Involved During the Quenching and Partitioning Process in Steels. In: *Metallurgical an Materials Transactions A*. Vol 42, no. 12, pp. 3620-3627

DOI: 10.21062/ujep/58.2018/a/1213-2489/MT/18/1/84